

Nanoscale

Accepted Manuscript



This is an *Accepted Manuscript*, which has been through the Royal Society of Chemistry peer review process and has been accepted for publication.

Accepted Manuscripts are published online shortly after acceptance, before technical editing, formatting and proof reading. Using this free service, authors can make their results available to the community, in citable form, before we publish the edited article. We will replace this *Accepted Manuscript* with the edited and formatted *Advance Article* as soon as it is available.

You can find more information about *Accepted Manuscripts* in the [Information for Authors](#).

Please note that technical editing may introduce minor changes to the text and/or graphics, which may alter content. The journal's standard [Terms & Conditions](#) and the [Ethical guidelines](#) still apply. In no event shall the Royal Society of Chemistry be held responsible for any errors or omissions in this *Accepted Manuscript* or any consequences arising from the use of any information it contains.

Ultra-Capacitor Flexible Films with Tailored Dielectric Constant using Electric Field Assisted Assembly of Nanoparticles

*Saurabh Batra, Miko Cakmak**

S. Batra, Dr., M. Cakmak, Prof.

Department of Polymer Engineering, The University of Akron, Akron, Ohio-44325, United States

E-mail: cakmak@uakron.edu

Keywords: Electric field, directed assembly, capacitors, flexible electronics, nanocomposite films.

In this study, the chaining and preferential alignment of barium titanate nanoparticles (100nm) through the thickness direction of polymer matrix in the presence of electric field is shown. Application of AC electric field in a well-dispersed solution leads to the formation of chains of nanoparticles in discrete rows oriented with their primary axis in the E-field direction due to dielectrophoresis. The change in orientation of these chains was quantified through statistical analysis of SEM images and was found to be dependent on E-field, frequency and viscosity. When DC field is applied a distinct layer consisting of dense particles was observed with micro-computed tomography. These studies show that with the increase in DC voltage leads to increase in thickness of the particle rich layer along with the packing density also increases. Increasing the mutual interactions between particles due to formation of particle chains in the “Z”-direction decreases the critical percolation concentration above which substantial enhancement of properties occur. This manufacturing method therefore shows a promise to lower the cost of the products for a range of applications including capacitors by either enhancing the dielectric properties for a given concentration or reduces the concentration of nanoparticles needed for a given property.

1. Introduction

Nanocomposites consists of two or more phases with at least one of phases in the nanometer scale range. Interest in these materials including polymer-metal,¹⁻³ polymer-glass,^{4,5} polymer-ceramic^{6,7} etc.⁸ have been primarily for the enhancement of properties of interest at low concentrations and/or low cost. Nanocomposites can also be differentiated with respect to their morphology or connectivity as has been described by Newnham in the late 70's.⁹ Newnham showed that multiphase composite connectivity plays an important role in the property enhancement of piezoelectric and pyroelectric materials and could lead to difference of several orders of magnitude in the final properties of nanocomposites depending on the connectivity present in the materials.¹⁰ In case of a composite with two phases taking into account that each phase can be self-connected in zero, two and three dimensions, ten different connectivities can be described. Thus, nanocomposites depend not only on the intrinsic properties of the matrix and particles but also on their morphology and interfacial characteristics. Traditional polymer processing techniques including extrusion, injection, blow molding etc. cannot efficiently create anisotropic networks of particles organized oriented morphologies in the thickness "Z" direction as they are primarily dominated by shear, extensional, biaxial or a combination these flows. To achieve directed assembly of such structures, external fields such as electric and magnetic fields¹¹ to enhance thickness properties useful for flexible electronics,^{12,13} membranes,¹⁴ supercapacitors,^{15,16} fuel cells,¹⁷ photovoltaics^{18,19} etc. Therefore, directed self-assembly techniques such as electric field assisted alignment are required. In the present work, we develop polymer nanocomposite films consisting of barium titanate (BaTiO₃) particles using electric field

assisted assembly to increase the organization and order of nanoparticles oriented in thickness direction for high power capacitors.

Barium titanate has been widely used as a raw material for electronic devices including multilayered capacitors,^{20,21} semiconductors,²² thermistors,²³ piezoelectric devices²⁴ and various other sensors.^{25–27} In addition to its high dielectric properties, BaTiO₃ is also thermally and chemically stable.²⁸ The dielectric properties of BaTiO₃ particles depend on their crystal structure. Tetragonal crystals exhibit higher dielectric constants when compared to cubic crystal structure. The crystal structure of BaTiO₃ particles depends on the temperature²⁹ and grain size.³⁰ It changes from tetragonal to cubic structure above the Curie temperature (~120⁰C) and with decrease in particle size (<100nm). However, in order to increase the efficacy of polymer composite systems and a continuous need to decrease the size of devices, smaller particle sizes are required. Therefore, we need to create devices with cubic BaTiO₃ maintaining the dielectric properties achieved by tetragonal particles.

Polymer nanocomposites consisting of ceramic nanoparticles as a filler represent a new class of engineering materials that shows a lot of promise as embedded and flexible capacitors^{31,32}. BaTiO₃ exhibits high dielectric constant, low dielectric loss and low dielectric breakdown³³, whereas polymers have high dielectric breakdown, ease of processability, low cost and flexibility.³⁴ Their composites offer properties that are useful for many current and future electronic applications such RFID tag antenna,³⁵ hybrid electric vehicles,³⁶ microwave,³⁷ flexible generators,³⁸ etc. Research in the past has been focused on investigating the energy storage capabilities of different materials and different compositions, and to achieve reasonably high energy storage or high dielectric constant nanocomposites often requires very high loading (>50 vol.%).³⁹ Higher loadings of ceramic particles leads to increase in dielectric properties but the

nanocomposites lose their flexibility, mechanical properties and dielectric breakdown strength. High volume fraction of particles also increases the weight of nanocomposite films due to the high density of ceramic particles; therefore, there is a need for nanocomposite films with lower filler loading to create cost effective and lightweight materials with enhanced properties. However, the dielectric properties depend on the percolation of particles in the matrix which can only be achieved at high volume fraction of filler loadings. Hence, these properties can only be enhanced by either controlling the morphology of the BaTiO₃ particles or by creating anisotropic nanocomposites. The connectivity and directional percolation of these particles can considerably increase the dielectric properties of even the nanocomposites with cubic particles and this is possible through electric field directed assembly techniques⁴⁰⁻⁴⁴.

These techniques have been used extensively in the past decade to create spatially and directionally oriented nanocomposites. During the application of a uniform electric field (AC) to a liquid with dielectric inclusions, dipole-dipole interactions occur. In this case, a polarization field of one particle disturbs the electric field at the center of the neighboring particles producing attractive and repulsive forces. This ultimately leads to chaining of particles creating anisotropic composites.^{40,45-47}

In this paper, results on the electric field driven alignment and accumulation of cubic barium titanate (BaTiO₃) nanoparticles are presented. The effect of electric field at different frequencies and particle concentrations creating z-oriented nanocomposites and formation of a layer consisting of highly dense particle layer is studied. Micro-morphological features particularly connectivity have been quantified to determine optimum composite and process parameters to maximize the desired properties to create flexible capacitor films with low filler loading to achieve high dielectric constants with low cost.

2. Results and Discussion

2.1. Characterization of BaTiO₃ Nanoparticles

BaTiO₃ particles used in this study were obtained with a particle size of 100nm. Scanning electron microscope (SEM) and transmission electron microscope (TEM) were used to determine the particle size, shape and morphology (Figure 1a and b). The particles were nearly spherical in shape and had an average particle size of $100\text{nm} \pm 15$. BaTiO₃ are unique perovskite crystals with high dielectric constants; however, the crystal structure rapidly changes from tetragonal to cubic with the decrease in particle size and increase in temperature. The crystal structure of these particles was determined by X-ray diffraction. In general, the difference between tetragonal and cubic phases can be confirmed by separation of (002) and (200) XRD peaks.³⁰ For the BaTiO₃ particles this peak is located at $2\theta = 45^\circ$. As can be seen from Figure 1d, there was only one observable peak at 45° which is attributed to the (200) plane, therefore, these particles were cubic in nature. Figure 1c shows the schematic of the cubic crystals of BaTiO₃.

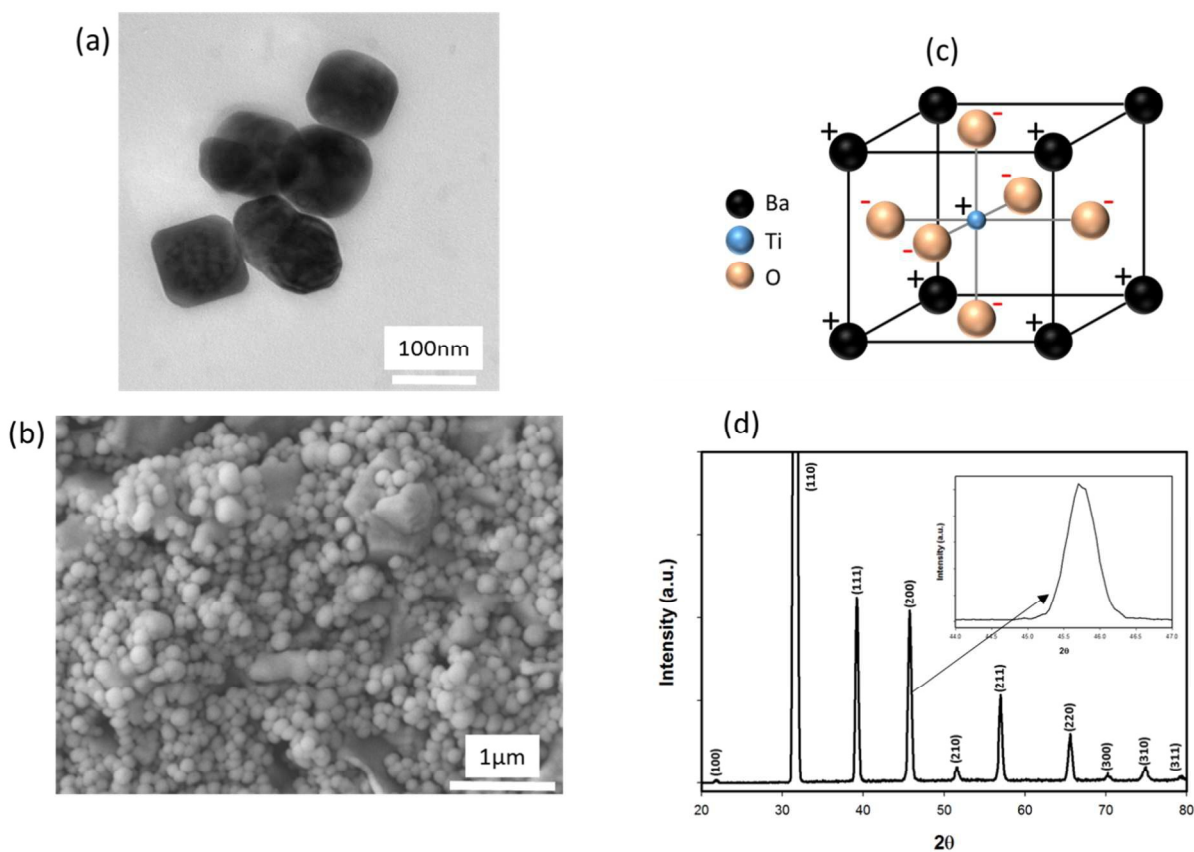


Figure 1. Characterization of 100nm BaTiO₃ nanoparticles, a) TEM, b) SEM showing morphology and c) schematic of the cubic structure of nanoparticles and d) X-ray diffraction pattern.

2.2. Electric field Manipulation

Electric field can be used to spatially arrange particles in a dielectric matrix using three techniques: electrophoresis,⁴⁸ electroosmosis⁴⁹ and dielectrophoresis.⁵⁰ The direction and magnitude of the force depends on the electric properties of the particle and the matrix along with their geometry. In this section, the effect of frequency, concentration and voltage on electric

field manipulation of the BaTiO₃ particles using electrophoresis and dielectrophoresis was discussed. Figure 14 shows the setup used for electric field manipulation.

Electrophoresis is the motion of a charged particle in an electric field and has been used considerably in industrial processes for electrophoretic deposition of uniform, high speed, high purity coatings⁵¹. This process is used to prepare coatings ranging from monolayer thickness to millimeter thick coatings with different self-assembly of particles. The process typically includes two electrodes dipped in an aqueous solution containing particles. Depending on the charge on the particles, applied electric field and application time these particles deposit on top of one of the electrodes.

An important parameter that is involved in all electrokinetic flows is known as zeta potential (ζ). Zeta potential is the potential at the slip plane that separates the bulk fluid from the boundary layer fluid⁵². This developed charges at slip plane between the boundary layer of particles and liquid medium with applied DC field leads to electrophoretic mobility, μ , and is defined as the coefficient of proportionality between the velocity and the applied field given by:

$$\mu = \frac{u}{E} \quad (1)$$

where, u is the velocity of particle under the applied electric field E . The electrophoretic mobility increases with increase in zeta potential and decreases with increase in viscosity (η) of the liquid medium. The electrophoretic mobility of the particles is thus defined by Helmholtz-Smoluchowski equation:

$$\mu = \frac{\varepsilon\varepsilon_0\zeta}{\eta} \quad (2)$$

In the following section, we will discuss the use of electrophoresis to create a micrometer thick and dense layer of particles in a flexible elastomeric film.

Dielectrophoresis is another alternative to manipulate particles in electric field and is caused by AC fields. The particles in a suspension with applied AC field are neither attracted nor repelled by the electrodes as the sign of the electrode polarization changes constantly. However, AC field leads to formation of induced dipoles on the particles leading to particle-particle interaction.⁵³ These induced dipoles also interact with the gradient of the field leading to dielectrophoretic force:⁵⁴

$$F_{DEP} = 2\pi\epsilon_m K r^3 \nabla E^2 \quad (3)$$

where, F_{DEP} is the dielectrophoretic force, ϵ_m is dielectric constant of matrix, K is the Clausius-Mossotti function, r is the radius of the particle and E is the applied field.

The sign and magnitude of the dielectrophoretic force depends on the effective polarizability of the particles which is given by real part of Clausius-Mossotti function (K):

$$K = \frac{\epsilon_p - \epsilon_m}{\epsilon_p + 2\epsilon_m} \quad (4)$$

where, ϵ_p , ϵ_m is the dielectric constant of the particle and matrix respectively.

Effect of Frequency on Alignment: Electric field alignment is highly dependent on the frequency of applied field. The ideal frequency depends on the particle and the fluid medium utilized, hence it is important to determine the ideal frequency range for each system. Figure 2 shows fractured cross-sectional images of the BaTiO₃ nanocomposites at different frequencies

showing alignment characteristics in the frequency range of DC, 10Hz–1kHz, at a constant applied voltage of 1400V/mm.

It was observed that the application of a DC voltage leads to the formation of a particle rich layer in the film, consisting of highly concentrated particles that are closely packed. However, applying AC voltage to the system led to the nanoparticle chain formation. At lower frequency of 10Hz and high frequency of 1000Hz, the observed chaining of particles was not very high. However, at 100Hz long chains of BaTiO₃ particles with the average chain length of 3-4μm were observed.

As the frequency decreases, the time between each cycle increases and thus low frequencies behave much like biased DC voltage. This causes the redistribution of ionic components in the charge layers near the electrodes, leading to space charge electrode polarization. Electrode polarization thus screens the potential drop in the suspension resulting in negligible dielectrophoretic forces.⁵⁵ However at higher frequency AC voltages, the effective polarization of the particles is not able to keep up with the applied changing field. This again leads to a transient dielectrophoretic force that is not enough to cause chaining of the particles in the matrix.

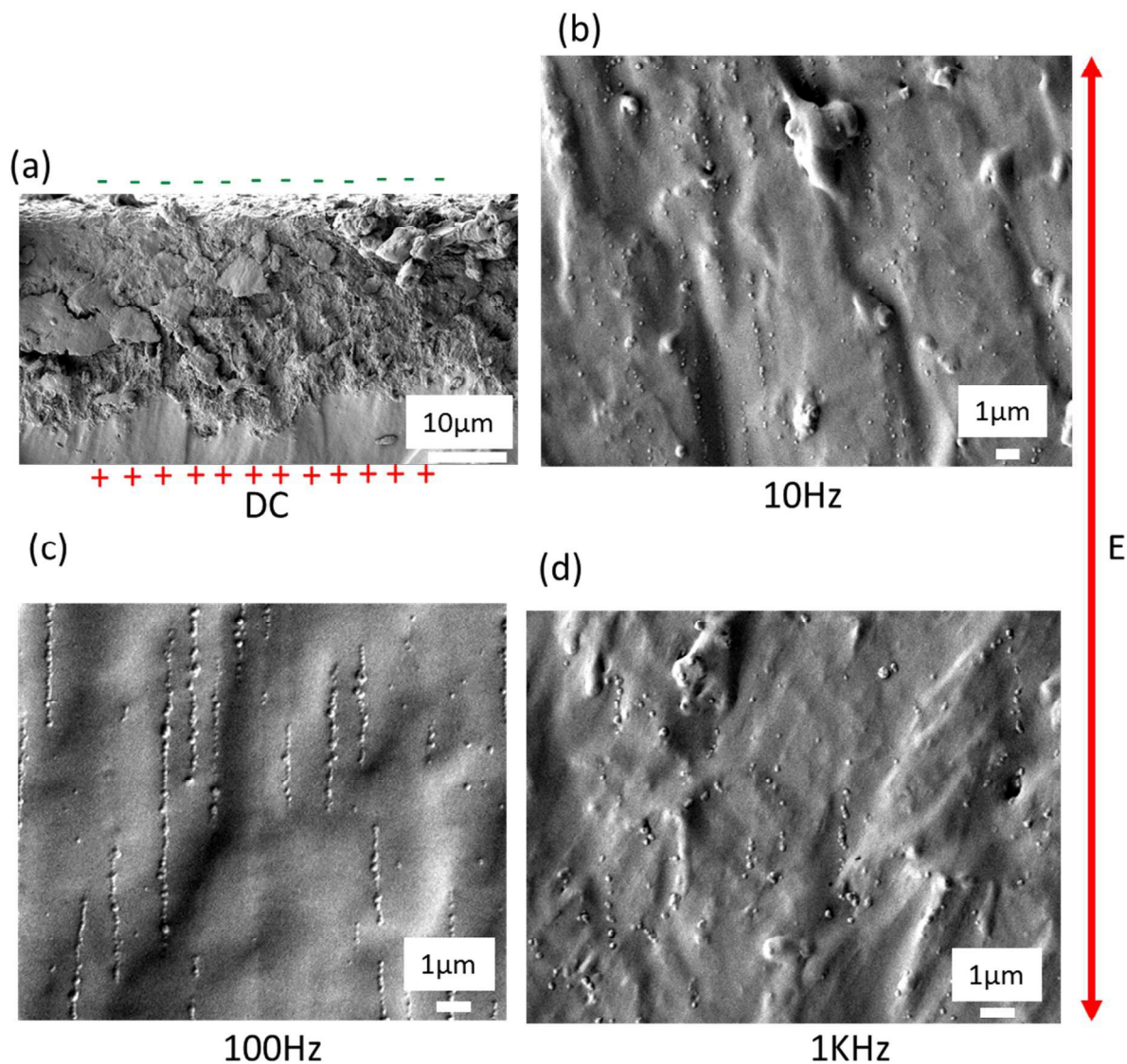


Figure 2. Effect of frequency at constant voltage (1400V/mm) on alignment characteristics of 10wt% BaTiO₃ nanoparticles in PDMS, a) DC, b) 10Hz, c) 100Hz d) 1KHz.

Formation of Particle Rich Layer: Electrophoretic deposition of BaTiO₃ nanoparticles in PDMS was studied at different voltages. The electrophoretic mobility of particles was highly dependent on the zeta potential of the particles. The zeta potential of the BaTiO₃ nanoparticles was

measured using a dilute dispersion of the particles in deionized water and was found to be negative ($\zeta = -26.3$ mV) with the electrophoretic mobility of -20.63 $\mu\text{m/s}$. The electrophoretic deposition was studied in 10wt% dispersion of BaTiO_3 nanoparticles in PDMS by applying varying DC voltages for 30 minutes. The dispersions were then cured for 2 hours with the applied voltage and the resulting film was used for further characterization.

As can be observed from Figure 3, the electrophoretic deposition of the particles in the polymer matrix led to the formation of dense particle layer in the film. This layer observed had a clear demarcation at the interface as can be seen in the higher magnification SEM images. The BaTiO_3 nanoparticles were deposited on the positive electrode indicating they are negatively charged in the dispersion, which is in agreement with the negative zeta potential measured earlier.

This particle rich layer observed in the SEM image was densely packed with the BaTiO_3 particles. With increasing voltage the layer thickness increased from $15\mu\text{m}$ at 300V/mm to $45\mu\text{m}$ at 1400V/mm as seen from Figure 3c. Thus, the thickness of the layer formed due to electrophoretic deposition is highly dependent on applied voltage and time of deposition, as has been shown by other researchers who have deposited nanoparticles from a colloidal solution onto an electrode.^{56,57} However, electrophoretic deposition has not been studied in detail in polymer films for the formation of particle rich layer with the application of voltage.

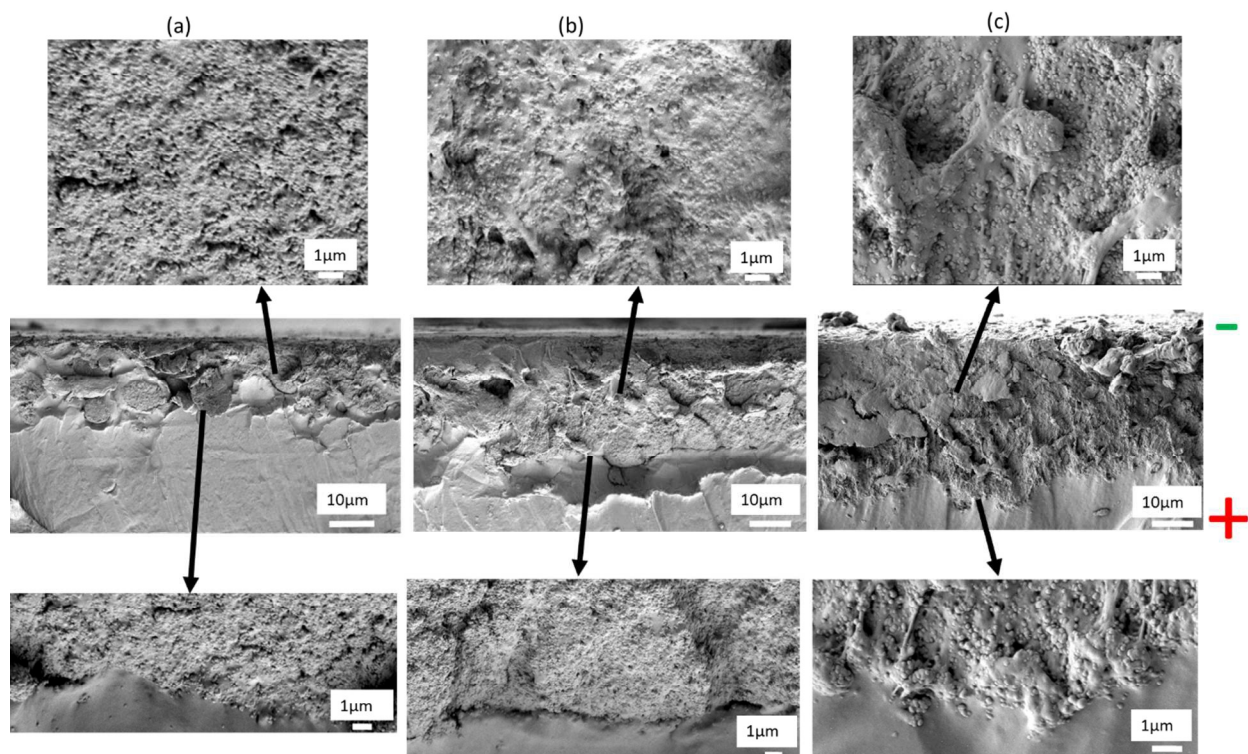


Figure 3. Formation of particle rich layer or the BaTiO₃ rich layer at different DC voltages a) 300V/mm, b) 800V/mm and c) 1400V/mm, the concentration of particles was kept constant at 10wt%.

During the formation of the layer due to electrophoretic deposition, voltage increases the layer thickness, however there is no experimental evidence regarding the packing structure or density for these nanoparticles. To understand the packing of the BaTiO₃ nanoparticles during electrophoretic deposition with varying voltages, X-ray microtomography was carried out. In Micro-CT, the X-ray images are stored while the sample is rotated. Internal structures are reconstructed as a series of 2D cross-section that are then used to analyze the two and three-dimensional morphology of the object. Ceramic particles like BaTiO₃ have density of 5.85 g/cm³, whereas the PDMS matrix has a density of 1.03 g/cm³. This density contrast leads to creation of spatial distribution of the particles and their arrangement in the films.

Figure 4a shows the false color images of 3D micro-CT experiments where the particle rich layer can be clearly observed. As the voltage during electrophoretic deposition was increased, the thickness of the layer increased and its color darkened. In addition, the layer became more compact with the increasing voltage indicating that the particles were more densely packed at higher voltages. The difference in packing density of the particles was also evident in the high magnification SEM images (Figure 3). This was an important finding that showed that higher voltages during electrophoretic deposition impact not only the thickness of the deposited layer but also its density gradient.

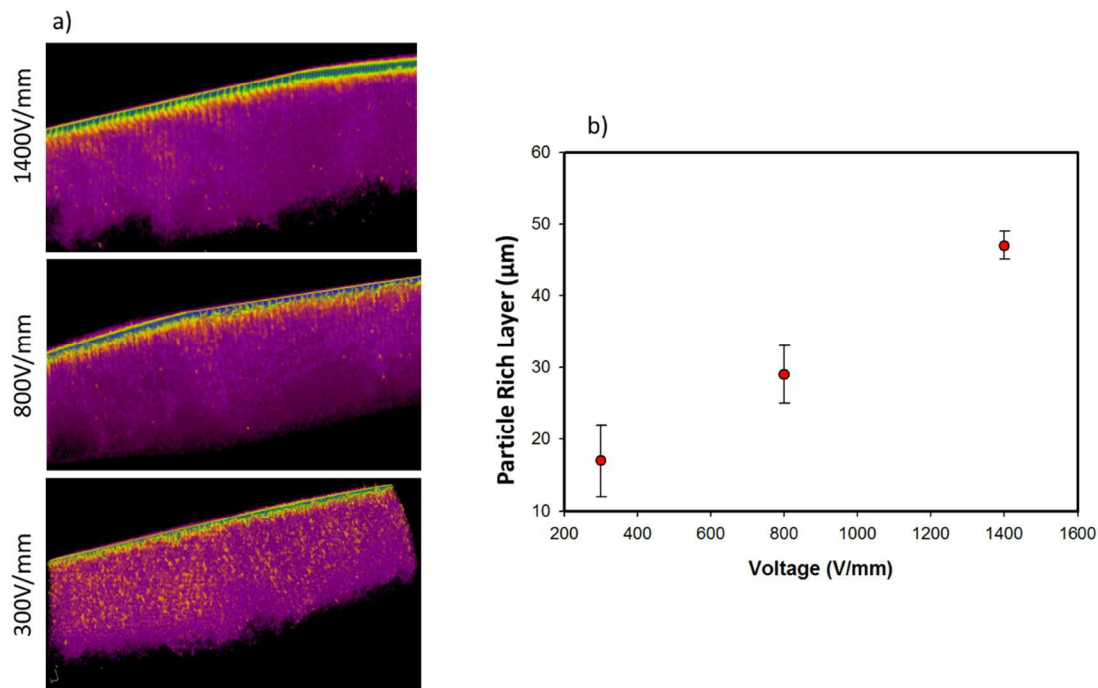


Figure 4. a) Micro-CT scans of 10wt.% BaTiO₃ nanocomposites aligned with DC voltage to observe the dense particle layer and b) average layer thickness.

Effect of Concentration and Voltage on Chaining: Dielectrophoresis leads to structuring of particles in the matrix between the two electrodes when a large number of particles are present in the suspension⁵⁸. The application of AC electric field leads to induced dipoles on the particles causing them to interact with each other if they are close enough, therefore producing attractive and repulsive forces between them. Hence, these induced particles interact with each other if they are close enough, producing attractive and repulsive forces. This ultimately leads to the formation of chains along the electric field lines resulting in maximum energy gain. The chaining force between the adjacent particles is dependent on the square of the electric field strength and square of the particle radius, and the equation is given by:⁵⁹

$$F_{chain} = -C\pi r^2 \epsilon_m K^2 E^2 \quad (5)$$

where, C is the coefficient ranging from 3 to 10^3 depending on the distance between particles and length of the particle chain,^{53,60} r is the radius of the particle, ϵ_m is the dielectric constant of the matrix, K is the Clausius-Mossotti function, and E is the applied field.

The chaining of particles in the BaTiO₃ nanocomposites was studied at 100Hz and an applied voltage of 1400V/mm at different concentrations of the BaTiO₃. As can be seen from the Figure 5, with the application of the AC field, BaTiO₃ chains were formed in the PDMS matrix. These chains were particularly long in the range of 3-5 micrometers at particle concentrations of 10 and 20wt.%; however with the increase in the particle concentration, the average chain length decreased considerably. At the extremely high 50wt% concentration, the average chain length was down to 400nm. This can be attributed to the decrease in particle mobility with the increase in particle concentration, as the viscosity increases considerably when the particle concentration is increased above 20 wt.% as can be seen in Figure 6. The dielectrophoretic force during the

particle chaining competes with the inertial and drag forces that increase with increase in viscosity. The mobility of the particles undergoing dielectrophoretic motion is inversely proportional to the viscosity and is given by the following equation:

$$v = \frac{\epsilon_m \epsilon_0 R^2 K}{12\pi\eta} \quad (6)$$

where, ϵ_m is the dielectric constant of the matrix, ϵ_0 is the permittivity of air, R is the radius of the particle, K is the Clausius-Mossotti function, and η is the viscosity of dispersion.

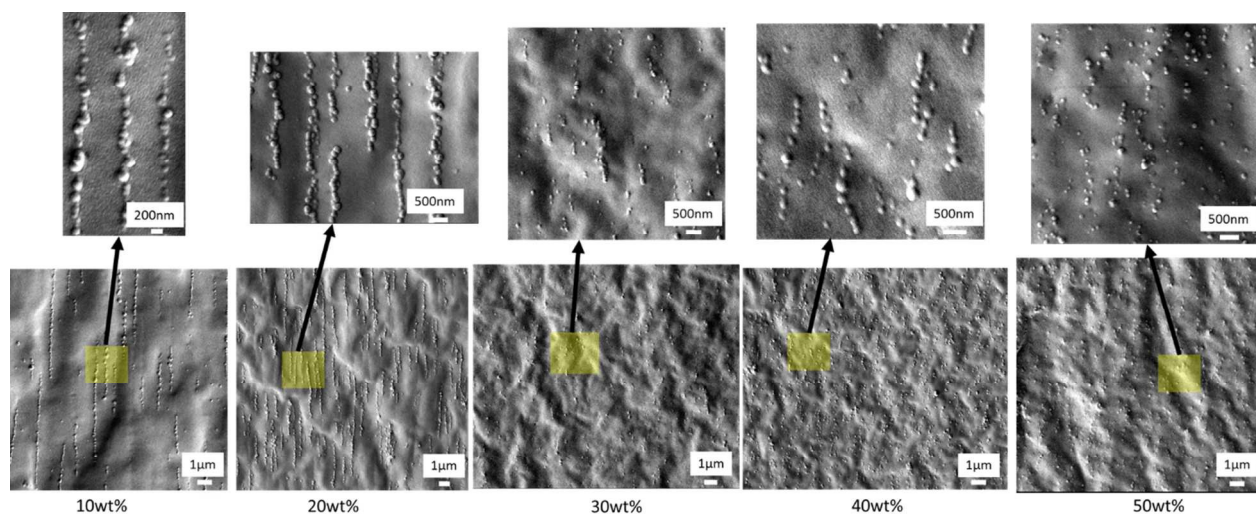


Figure 5. Concentration effect on alignment of BaTiO₃ nanoparticles at 1400V/mm and 100Hz, a) 10wt%, b) 20wt%, c) 30wt%, d) 40wt%, e) 50wt%.

Thus, as the viscosity of the matrix is increased with particle concentration, the mobility of the particles decreased leading to formation of shorter chains. Also with the increase in particle loading, there was an increased frustration between the particles because of restricted motion to form long chains. As a result, reduction in the distance between the chains and also the order of

the chains was observed. As can be seen from Figure 5, at lower particle concentration, the particle chains were much farther apart and almost parallel to the direction of applied field. However, increasing concentration led to skewed chains and reduction in the distance between the adjacent chains.

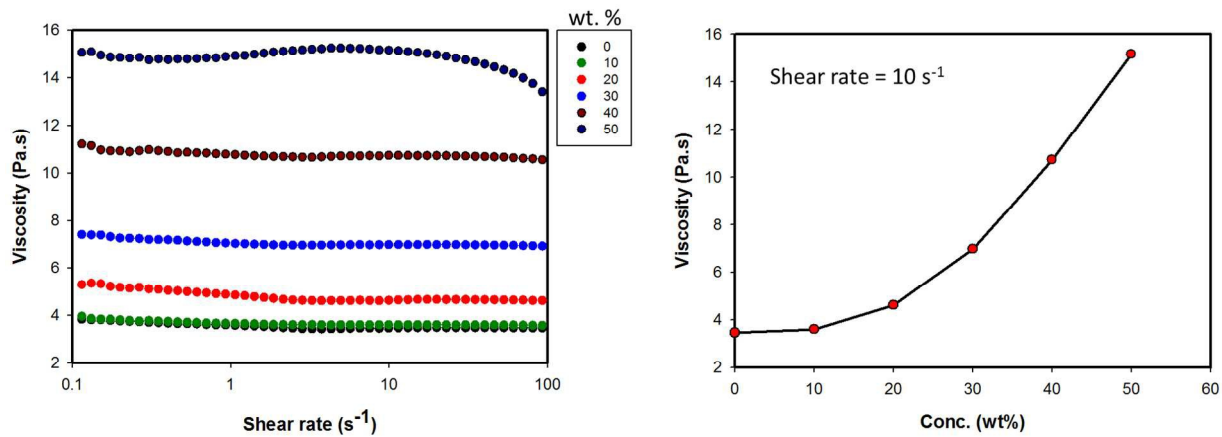


Figure 6. Concentration effect of BaTiO₃ nanoparticles on viscosity of dispersion.

To quantify the alignment characteristics due to dielectrophoresis, statistical analysis of various parameters including chain length, distance between the chains, and the angle of orientation with respect to the applied electric field using multiple SEM images at different sample locations was performed. A sample size of 100 was used for the statistical analysis. Figure 7 shows the analysis for three different concentrations of BaTiO₃ nanocomposites. For this analysis, the 100 chains chosen consisted of at least three or more particles.

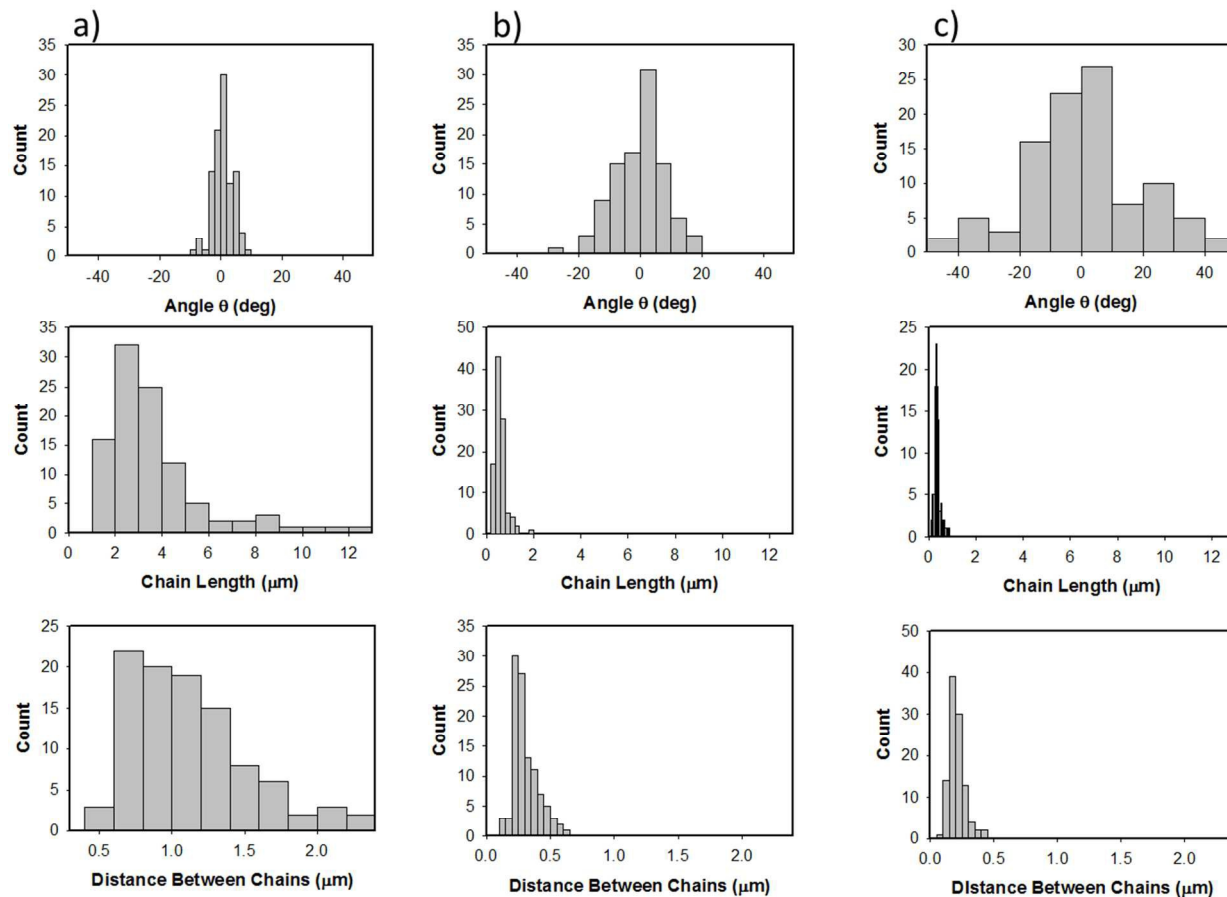


Figure 7. Statistical analysis of chaining characteristics including angle of orientation with respect to electric field direction, chain length, and distance between the two chains at different concentrations a) 10wt%, b) 20wt% and c) 30wt% of dielectrophoretically aligned BaTiO₃ nanocomposites at 1400V/mm.

To determine the orientation factor using the statistical analysis, we defined the order parameter S . If θ is the angle of a chain with respect to the electric field, the order parameter was determined by averaging the orientation angles of all chains according to:

$$S = \frac{(3\cos^2\theta - 1)}{2} \quad (7)$$

The two limiting values from the above equation are i) $S = 1$, in the case of perfect alignment where all chains are parallel to the direction of electric field and ii) $S = -0.5$, if the chains are perpendicular to the field.

Thus, the average orientation of the chains was quantified from the SEM images by averaging more than 100 samples. For the control experiments *i.e.* without the application of any electric field, there was no chain formation and all the particles were uniformly dispersed, hence the orientation parameter cannot be calculated.

The order parameter as a function of concentration plotted in Figure 8 (red curve). The orientation factors for lower particle concentration of 10 and 20wt% remained almost constant and were very close to perfect alignment with $S = 0.99$. As the concentration is increased, orientation factor decreased to $S = 0.86$ for 50 wt.% particle concentration. This was due to the restriction of motion at high particle concentration and viscosity as has been discussed above.

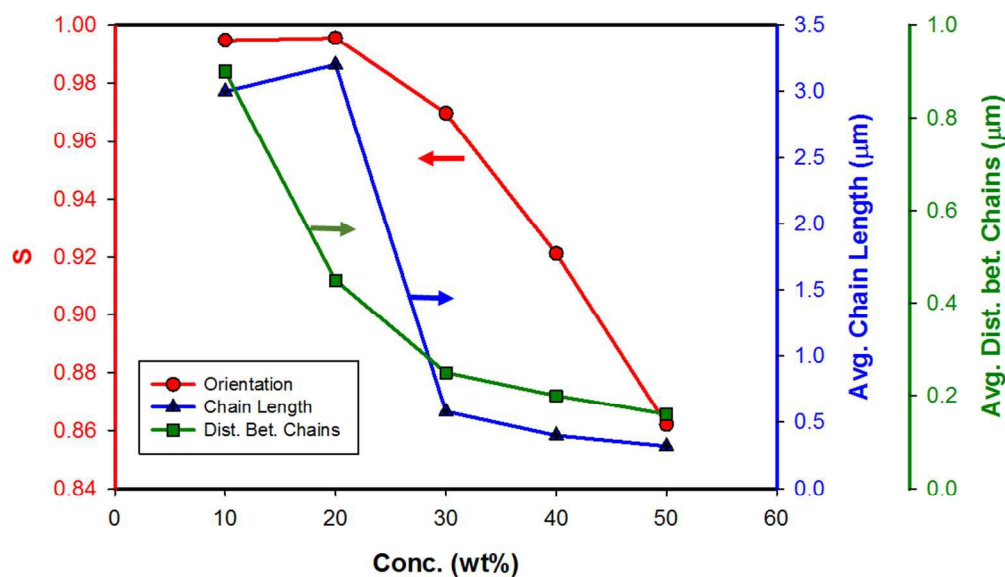


Figure 8. Change in orientation factor (S), chain length and distance between chains as a function of concentration.

Dielectrophoresis of particles caused both attractive and repulsive forces, which led to the chaining of particles as can be seen in Figure 9a and Figure 9b. In the current study, the chains of BaTiO₃ nanoparticles comprised of single particles attached to each other with a uniform distance between two chains, as can be seen from the statistical analysis shown in Figure 7. The distance between the two chains ($2d$) is depicted in Figure 9c. Half of this distance (d) can be called as a depletion layer, which means that a particle present in this zone will attach to the closest chain resulting in absence of particles in this region. As seen from Figure 8, the depletion zone decreased with increase in particle concentration from 450 nm to around 80 nm. This was caused due to three factors: the first two as discussed above were restriction of motion due to increased viscosity, and particle frustration⁶¹. The third factor was the increase in particle density

with increased concentration. With the increase in the volume fraction, the particles were inherently much closer to each other leading to particle-particle interaction and causing the depletion layer to decrease.

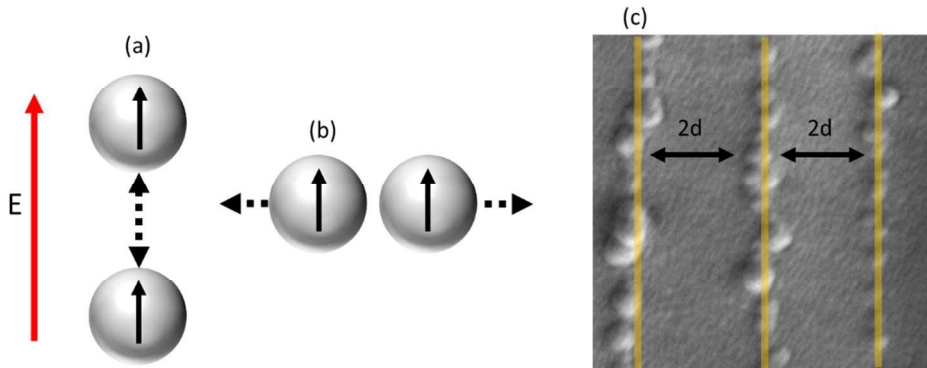


Figure 9. Schematic of a) attractive and b) repulsive forces during dielectrophoretic alignment and c) showing depletion layer d in an aligned BaTiO_3 nanocomposite.

Chaining was also studied at different voltages keeping the concentration of the particles fixed at 20wt%, as shown in Figure 10. It was observed that at 300V/mm, there was no formation of chains in the BaTiO_3 nanocomposites. As the voltage increased from 300 V/mm to 800 V/mm, chains were formed although not fully developed. At 1400 V/mm, the chains were fully developed and this was due to increase in the dipole moment which is directly proportional to the square of the voltage.

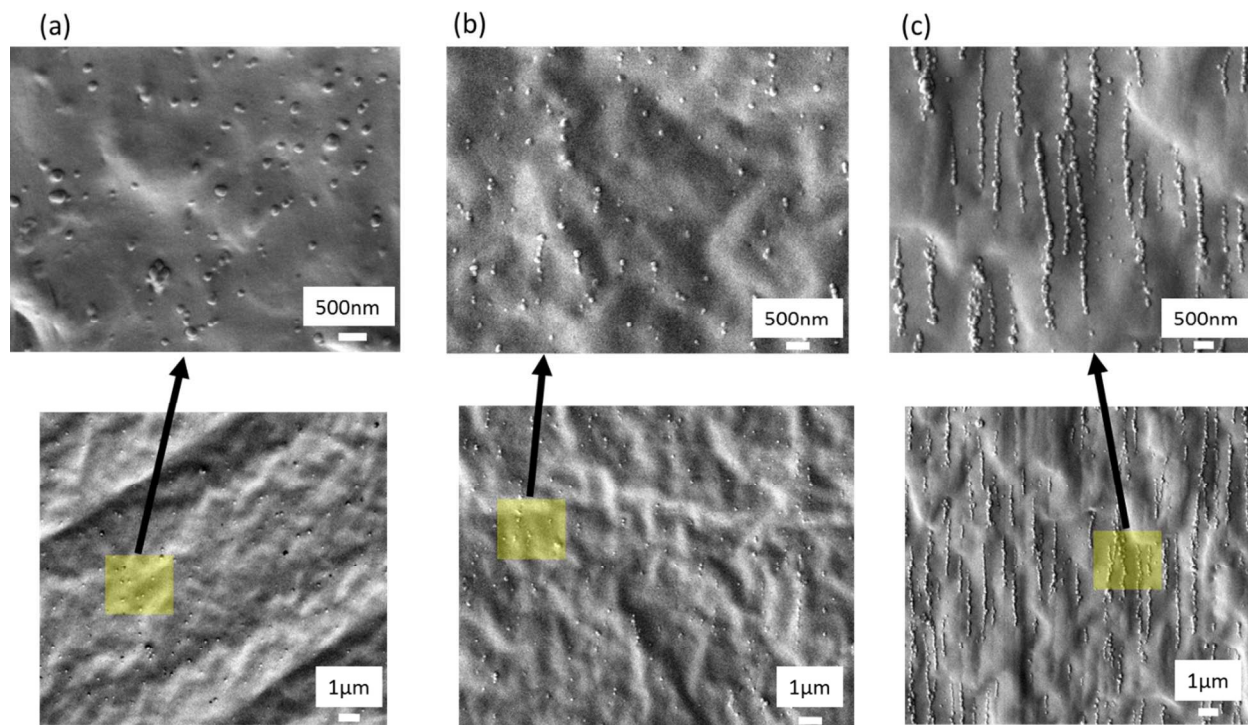


Figure 10. Chaining of BaTiO₃ at different AC (100Hz) voltages a) 300V/mm, b) 800V/mm and c) 1400V/mm. The concentration of particles was kept constant at 20wt%.

2.3. Dielectric Properties of Aligned Nanocomposite Film:

We demonstrate the enhancement in the Z-direction properties of BaTiO₃ nanocomposite films using dielectric measurements. The dielectric properties of both oriented and unoriented films were measured through the thickness of the film. All the oriented film samples were subjected to 1400 V/mm. Figure 11 compares the dielectric permittivity and dielectric loss of unoriented and oriented samples at room temperature. The dielectric constant above 0.1 Hz remains constant, however it starts increasing below 0.1 Hz for oriented systems as compared to unoriented systems as the nanocomposites incorporate more ionic dipoles in the direction of measurement

leading to ionic polarization. It can be seen the dielectric properties are enhanced with addition of BaTiO₃ nanoparticles and also with the alignment of nanoparticles.

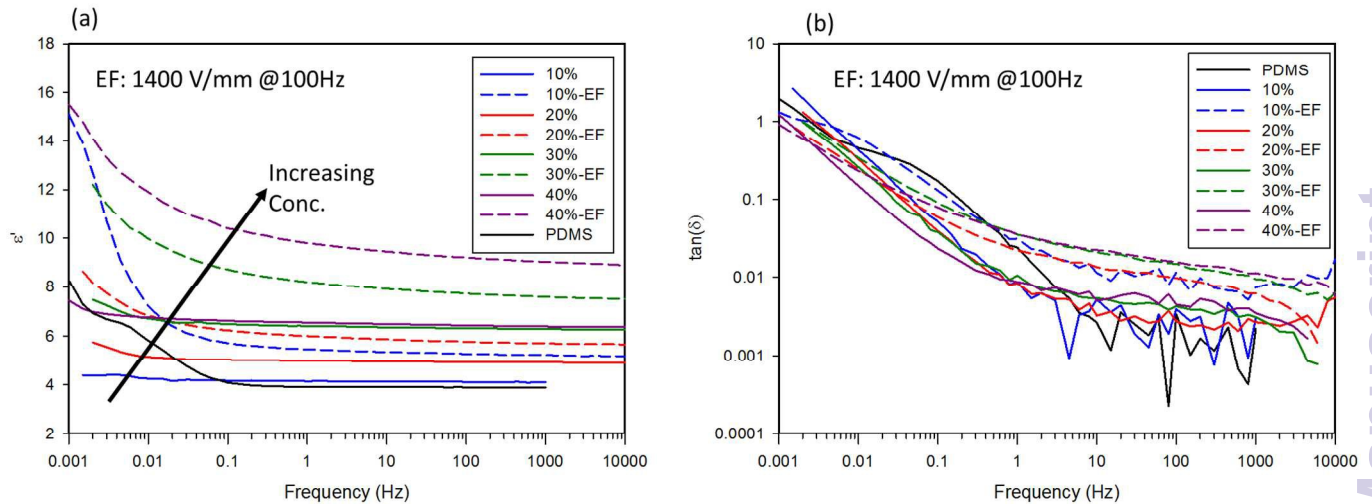


Figure 11. Change in a) dielectric constant and b) dielectric loss for oriented and unoriented nanocomposite films of BaTiO₃. (EF: Electric field oriented films)

Figure 12 compares three films at same concentration of particles (10wt%), including the unoriented films, oriented films with BaTiO₃ chains using dielectrophoresis and phase separated films with particle rich layer consisting. The dielectric properties of aligned composite was observed to be higher when compared to the particle rich layer and the unoriented sample.

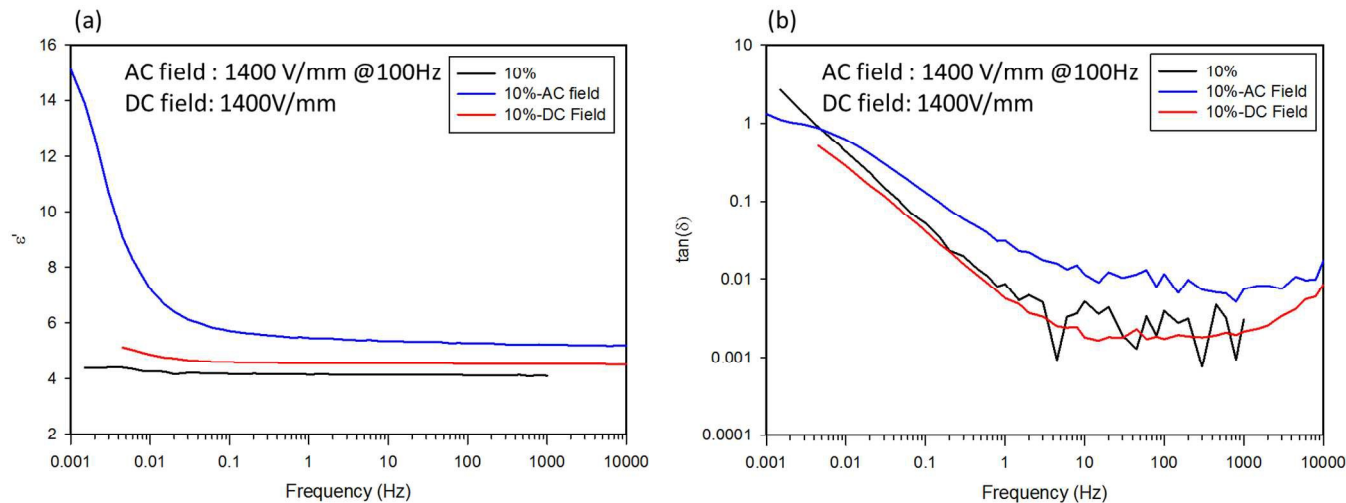


Figure 12. Difference between a) dielectric constant and b) dielectric loss for oriented samples using dielectrophoresis and particle rich layer formation in electrophoresis.

Figure 13 shows the dielectric properties of films produced by different routes are compared at 10Hz. The dielectric constant of pure matrix is 3.9 and increases with addition of BaTiO₃ nanoparticles to 6.3 till 30wt%, however with further increase of nanoparticle concentration only slight increase in dielectric constant was observed. However, for the oriented films which are directionally percolated there is an increased interaction between the particles thus showing much higher dielectric constant of 9.5 with only 40wt% particle concentration. Hence, alignment of particles increases the dielectric properties considerably, therefore, less amount of nanoparticles are required to achieve the similar dielectric properties. It should also be noted that dielectric loss tangent increases with increase in concentration for oriented samples, which can be attributed to the electrode polarization caused by alignment of particles. However, the dielectric loss remains constant for unoriented samples.

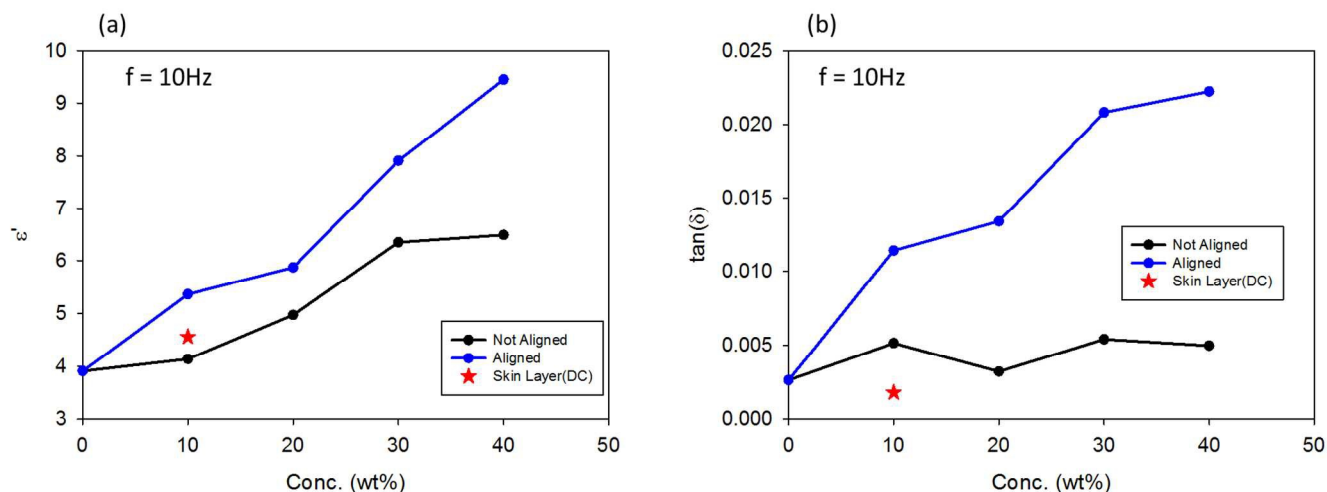


Figure 13. Increase in a) dielectric constant and b) dielectric loss for oriented nanocomposite films of BaTiO₃.

3. Conclusions

The electric field application allows Z-(thickness direction) alignment and organization of nanoparticles in polymer matrix, facilitating the tailoring of properties in this direction. In this study, results on the quantitative analysis of dielectrophoretic chaining of barium titanate particles in a polymer matrix have been demonstrated. At low particle concentration, chains of particles up to 5 microns in length were obtained consisting of 35-45 particles per chain. The orientation, chain length and depletion zone of the chained particles decreased with increase in viscosity. Electrophoresis of the particles inside the polymer matrix was also shown for the formation of densely packed particle layer in DC field. The thickness of the layer decreased with increasing voltage. Micro-CT experiments revealed that increasing voltage also resulted in decreased packing density. Aligned nanoparticles show considerable enhancement in their dielectric properties, nanocomposite films show upto 30% increase in dielectric properties for oriented nanocomposite samples.

4. Experimental Section

4.1 Materials

BaTiO₃ nanoparticles with an average particle size of 100nm were obtained from US Research Nanomaterials, Inc., Houston, TX. A thermally curable resin polydimethylsiloxane (PDMS), Sylgard 184 was obtained from Dow Corning Co., Midland, MI and used as the matrix to prepare aligned nanocomposites. Sylgard 184 silicone elastomer is a two-part system consisting of monomer and cross linker mixed in a 10:1 ratio. It is a solvent free resin and can be cured at 80⁰C for 1hr. Operating temperature range for the PDMS is from -45 to 200⁰C. Along with flexibility, it has high dielectric strength, shear stability and good UV resistance. The BaTiO₃ particles and the PDMS matrix were used without further modification. Indium Tin Oxide (ITO) coated glasses obtained from SPI Supplies, West Chester, PA were used as electrodes for electric field assisted alignment.

4.2 Preparation of ordered nanocomposite films using Electric field

To prepare aligned polymer nanocomposites, BaTiO₃ particles at a range of concentrations were dispersed in the PDMS resin using Thinky Planetary Centrifugal Mixer ARV-310 to achieve reproducible dispersions for all samples. The cross linker was added to the dispersions and the samples were then placed in a vacuum oven for 10 min. for degassing. A cell consisting of two ITO coated glass electrodes separated by 1mm spacer was prepared as shown in Figure 1. The top electrode was connected to high voltage amplifier Matsuda 20B20 which was connected to H-P function generator and the bottom electrode was grounded. The suspensions were then loaded in the cell kept on a hot plate. Electric field was applied between the two electrodes for 30

min and the morphology of the resulting nanocomposites was frozen by heating the sample at 80°C for two hours.

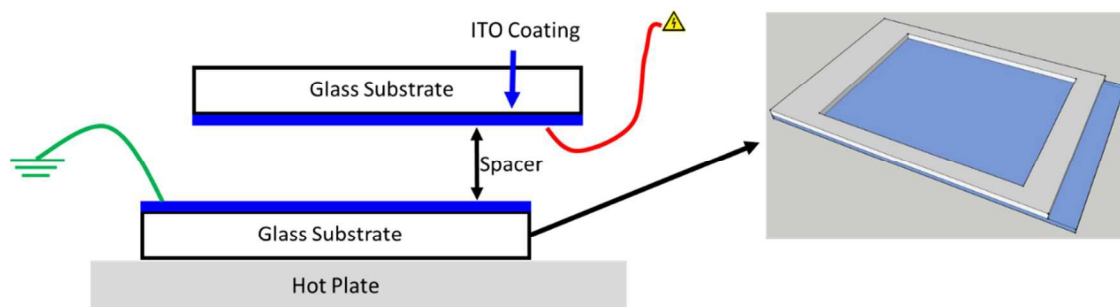


Figure 14. Schematic of the setup used for the electric field assisted alignment.

4.3 Characterization

X-Ray Diffraction: The crystal structure of the BaTiO₃ nanoparticles was determined using Bruker AXS D8 Goniometer generator equipped with a copper tube and a two dimensional detector. The generator was operated at 40kV and 40mA with a beam monochromatized to CuK_α radiation ($\lambda=0.1542\text{nm}$). A typical exposure time of 10 min was used for measurements.

Scanning Electron Microscope: The morphology of the BaTiO₃ powder and fractured surfaces of cured films were characterized using a high resolution Scanning electron microscope (JEOL JSM 5310; SEM). The nanocomposites were brittle fractured under liquid nitrogen followed by sputter coating by silver before SEM characterization. The operating voltage and current used were 1kV and 20mA.

Transmission Electron Microscope: BaTiO₃ powders were also characterized using a JEOL-1230 transmission electron microscope (TEM) with an accelerating voltage of 120kV. TEM images were taken using a digital CCD camera and processed with the accessory digital imaging system.

Zeta Potential: The zeta-potential measurement was conducted using a Malvern Instrument (Nano ZS90) equipped with a 632.8-nm He-Ne laser. The instrument calculated the zeta potential by determining the electrophoretic mobility and applying the Henry equation (equation 1).

$$U_E = \frac{2\varepsilon_m \zeta f(Ka)}{3\eta} \quad (8)$$

Where, U_E is the electrophoretic velocity, ε_m is the dielectric constant of the medium, ζ is the zeta potential, $f(Ka)$ is the correction function and η is the viscosity. The electrophoretic mobility was obtained by performing an electrophoresis experiment on the sample and measuring the velocity of the particles using a laser Doppler velocimeter.

Micro-CT: A high resolution micro-CT Skyscan 1172 was used to determine the thickness of the particle rich (dense) layer during the electric field alignment using a DC voltage. This layer was easily observable in the micro-CT due to high contrast in density between the BaTiO₃ particles and the polymer matrix.

Acknowledgements

We gratefully acknowledge the funding from Third Frontier, Wright Center of Innovation program (CMPND) of The State of Ohio. We would like to thank JoAnne Ronzello from University of Connecticut for dielectric spectroscopy measurements.

Received: ((will be filled in by the editorial staff))

Revised: ((will be filled in by the editorial staff))

Published online: ((will be filled in by the editorial staff))

- 1 V. Varadan, A. Pillai, D. Mukherji, M. Dwivedi and L. Chen, *Nanoscience and nanotechnology in engineering*, 2010.
- 2 L. Nicolais and G. Carotenuto, *Metal-polymer nanocomposites*, 2004.
- 3 P. Xu, X. Han, B. Zhang, Y. Du and H.-L. Wang, *Chem. Soc. Rev.*, 2014, **43**, 1349–60.
- 4 B. Sharma, S. Mahajan, R. Chhibber and R. Mehta, *Procedia Chem.*, 2012, **4**, 39–46.
- 5 W. M. Chiridon, W. J. O'Brien and R. E. Robertson, *Dent. Mater.*, 2006, **22**, 57–62.
- 6 a C. Patsidis and G. C. Psarras, *Smart Mater. Struct.*, 2013, **22**, 115006.
- 7 C.-Y. Liu and A. J. Bard, *Chem. Mater.*, 2000, **12**, 2353–2362.
- 8 F. Gao, *Advances in polymer nanocomposites: Types and applications*, 2012.
- 9 R. E. Newnham, D. P. Skinner and L. E. Cross, *Mater. Res. Bull.*, 1978, **13**, 525–536.

- 10 E. Ionescu, H.-J. Kleebe and R. Riedel, *Chem. Soc. Rev.*, 2012, **41**, 5032–52.
- 11 M. Cakmak, S. Batra and B. Yalcin, *Polym. Eng. Sci.*, 2014.
- 12 D. a Kunz, J. Schmid, P. Feicht, J. Erath, A. Fery and J. Breu, *ACS Nano*, 2013, **7**, 4275–80.
- 13 A. M. Marconnet, N. Yamamoto, M. a Panzer, B. L. Wardle and K. E. Goodson, *ACS Nano*, 2011, **5**, 4818–25.
- 14 B. R. Vaughan and E. Marand, *J. Memb. Sci.*, 2008, **310**, 197–207.
- 15 H. Lin, L. Li, J. Ren, Z. Cai, L. Qiu, Z. Yang and H. Peng, *Sci. Rep.*, 2013, **3**, 1353.
- 16 Y. Zhang, Y. Wang, Y. Deng, Y. Guo, W. Bi, M. Li, Y. Luo and J. Bai, *Appl. Phys. Lett.*, 2012, **101**, 192904.
- 17 D. Yuan, Z. Liu, S. W. Tay, X. Fan, X. Zhang and C. He, *Chem. Commun. (Camb.)*, 2013, **49**, 9639–41.
- 18 W. Huynh, J. Dittmer, N. Teclemariam, D. Milliron, A. Alivisatos and K. Barnham, *Phys. Rev. B*, 2003, **67**, 115326.
- 19 C. I. Pelligra, P. W. Majewski and C. O. Osuji, *Nanoscale*, 2013, **5**, 10511.
- 20 O. Guillon, J. Chang, S. Schaab and S.-J. L. Kang, *J. Am. Ceram. Soc.*, 2012, **95**, 2277–2281.
- 21 T. Schneller, S. Halder, R. Waser, C. Pithan, J. Dornseiffer, Y. Shiratori, L. Houben, N. Vyshnavi and S. B. Majumder, *J. Mater. Chem.*, 2011, **21**, 7953.
- 22 K. Maeda, *ACS Appl. Mater. Interfaces*, 2014, **6**, 2167–73.
- 23 D. S. Smith, N. Ghayoub, I. Charissou, O. Bellon, P. Abélard and A. H. Edwards, *J. Am. Ceram. Soc.*, 2005, **81**, 1789–1796.
- 24 Y. Huan, X. Wang, J. Fang and L. Li, *J. Am. Ceram. Soc.*, 2013, **96**, 3369–3371.

- 25 R. Popielarz, C. K. Chiang, R. Nozaki and J. Obrzut, *Macromolecules*, 2001, **34**, 5910–5915.
- 26 S. R. Kwon, W. B. Huang, S. J. Zhang, F. G. Yuan and X. N. Jiang, *Smart Mater. Struct.*, 2013, **22**, 115017.
- 27 D. Hennings, M. Klee and R. Waser, *Adv. Mater.*, 1991, **3**, 334–340.
- 28 X. Huang, Z. Pu, L. Tong, R. Zhao and X. Liu, *J. Electron. Mater.*, 2013, **42**, 726–733.
- 29 X. Li and W.-H. Shih, *J. Am. Ceram. Soc.*, 1997, **80**, 2844–2852.
- 30 W. Sun, *J. Appl. Phys.*, 2006, **100**, 083503.
- 31 K.-I. Park, S. Y. Lee, S. Kim, J. Chang, S.-J. L. Kang and K. J. Lee, *Electrochem. Solid-State Lett.*, 2010, **13**, G57.
- 32 Y. Song, Y. Shen, H. Liu, Y. Lin, M. Li and C.-W. Nan, *J. Mater. Chem.*, 2012, **22**, 8063.
- 33 K. Nair, *Advances in Electroceramic Materials: Ceramic Transactions*, 2009.
- 34 X. Zhou, X. Zhao, Z. Suo, C. Zou, J. Runt, S. Liu, S. Zhang and Q. M. Zhang, *Appl. Phys. Lett.*, 2009, **94**, 162901.
- 35 Y. Zhou, S. Koulouridis, G. Kiziltas and J. Volakis, *Antennas Wirel. Propag. Lett.*, 2006, **5**, 224–227.
- 36 P. Barber, S. Balasubramanian, Y. Anguchamy, S. Gong, A. Wibowo, H. Gao, H. J. Ploehn and H.-C. zur Loye, *Materials (Basel)*, 2009, **2**, 1697–1733.
- 37 S. Koulouridis, G. Kiziltas, Y. Zhou, D. J. Hansford and J. L. Volakis, *IEEE Trans. Microw. Theory Tech.*, 2006, **54**, 4202–4208.
- 38 K.-I. Park, M. Lee, Y. Liu, S. Moon, G.-T. Hwang, G. Zhu, J. E. Kim, S. O. Kim, D. K. Kim, Z. L. Wang and K. J. Lee, *Adv. Mater.*, 2012, **24**, 2999–3004, 2937.

- 39 Y. C. Li, *Express Polym. Lett.*, 2011, **5**, 526–534.
- 40 D. a. van den Ende, S. E. van Kempen, X. Wu, W. a. Groen, C. a. Randall and S. van der Zwaag, *J. Appl. Phys.*, 2012, **111**, 124107.
- 41 K. D. Hermanson, S. O. Lumsdon, J. P. Williams, E. W. Kaler and O. D. Velev, *Science*, 2001, **294**, 1082–6.
- 42 V. Olszowka, M. Hund, V. Kuntermann, S. Scherdel, L. Tsarkova and A. Böker, *ACS Nano*, 2009, **3**, 1091–6.
- 43 E. S. Choi, J. S. Brooks, D. L. Eaton, M. S. Al-Haik, M. Y. Hussaini, H. Garmestani, D. Li and K. Dahmen, *J. Appl. Phys.*, 2003, **94**, 6034.
- 44 T. Prasse, *Compos. Sci. Technol.*, 2003, **63**, 1835–1841.
- 45 T. C. Halsey, *Science (80-.)*, 1992, **258**, 761–6.
- 46 G. Kim and Y. M. Shkel, *J. Mater. Res.*, 2004, **19**, 1164–1174.
- 47 A. Ramos, H. Morgan, N. G. Green and A. Castellanos, *J. Phys. D. Appl. Phys.*, 1998, **31**, 2338–2353.
- 48 L. Besra and M. Liu, *Prog. Mater. Sci.*, 2007, **52**, 1–61.
- 49 S. Ghosal, *Electrophoresis*, 2004, **25**, 214–28.
- 50 R. Pethig, *Biomechanics*, 2010, **4**.
- 51 C. P. Gutierrez, J. R. Mosley and T. C. Wallace, *J. Electrochem. Soc.*, 1962, **109**, 923.
- 52 J. Lyklema, *J. Colloid Interface Sci.*, 1977, **58**, 242–250.
- 53 O. D. Velev and K. H. Bhatt, *Soft Matter*, 2006, **2**, 738.
- 54 H. Pohl, *Dielectrophoresis: the behavior of neutral matter in nonuniform electric fields*,

Cambridge university press Cambridge, 1978.

- 55 C. P. Bowen, T. R. ShROUT, R. E. Newnham and C. a. Randall, *J. Mater. Res.*, 2011, **12**, 2345–2356.
- 56 R.-F. Louh and Y.-H. Hsu, *Mater. Chem. Phys.*, 2003, **79**, 226–229.
- 57 J. Q. Wang and M. Kuwabara, *J. Eur. Ceram. Soc.*, 2008, **28**, 101–108.
- 58 C. Randall, S. Miyazaki, K. More, A. S. Bhalla and R. E. Newnham, *Mater. Lett.*, 1992, **15**, 26–30.
- 59 T. B. Jones, *Electromechanics of particles*, Cambridge Univ Pr, 2005.
- 60 O. D. Velev, S. Gangwal and D. N. Petsev, *Annu. Reports Sect. 'C' (Physical Chem.)*, 2009, **105**, 213.
- 61 S. Batra, E. Unsal and M. Cakmak, *Adv. Funct. Mater.*, 2014, **24**, 7698–7708.